The Plant Cell, Vol. 30: 2779–2794, November 2018, www.plantcell.org © 2018 ASPB.

Transcriptional Regulation of the Immune Receptor FLS2 Controls the Ontogeny of Plant Innate Immunity

Yanmin Zou,[a,1] Shuangfeng Wang,[a,b,1] Yuanyuan Zhou,[a,b] Jiaojiao Bai,[a,b] Guozhong Huang,[a,b] Xiaotong Liu,[a] Yingying Zhang,[a] Dingzhong Tang,[c] and Dongping Lu[a,2]

[a]State Key Laboratory of Plant Genomics, Center for Agricultural Resources Research, Institute of Genetics and Developmental Biology, Chinese Academy of Sciences, Shijiazhuang, Hebei 050021, China
[b]University of the Chinese Academy of Sciences, Beijing 100049, China
[c]Key Laboratory of the Ministry of Education for Genetics, Breeding, and Multiple Utilization of Crops, Fujian Agriculture and Forestry University, Fuzhou 350002, China

ORCID IDs: 0000-0002-4609-6277 (Y.Z.); 0000-0003-3463-0361 (S.W.); 0000-0001-5688-9804 (Y.Z.); 0000-0002-8919-8329 (J.B.); 0000-0002-9150-6802 (G.H.); 0000-0002-9256-297X (X.L.); 0000-0002-3117-2855 (Y.Z.); 0000-0001-8850-8754 (D.T.); 0000-0002-4888-0532 (D.L.)

Innate immunity plays a vital role in protecting plants and animals from pathogen infections. Immunity varies with age in both animals and plants. However, little is known about the ontogeny of plant innate immunity during seedling development. We report here that the Arabidopsis (*Arabidopsis thaliana*) microRNA miR172b regulates the transcription of the immune receptor gene *FLAGELLIN-SENSING2* (*FLS2*) through TARGET OF EAT1 (TOE1) and TOE2, which directly bind to the *FLS2* promoter and inhibit its activity. The level of miR172b is very low in the early stage of seedling development but increases over time, which results in decreased TOE1/2 protein accumulation and, consequently, increased *FLS2* transcription and the ontogeny of FLS2-mediated immunity during seedling development. Our study reveals a role for the miR172b-TOE1/2 module in regulating plant innate immunity and elucidates a regulatory mechanism underlying the ontogeny of plant innate immunity.

INTRODUCTION

Plant innate immunity represents the first line of inducible host defense against pathogens (Jones and Dangl, 2006; Takeuchi and Akira, 2010). FLAGELLIN-SENSING2 (FLS2), a well-studied plasma membrane-localized leucine-rich repeat receptor-like kinase (LRR-RLK), recognizes the pathogen-associated molecular pattern (PAMP) flagellin or its derived peptide flg22 to mount PAMP-triggered immunity (PTI) (Gómez-Gómez and Boller, 2000; Jones and Dangl, 2006). The perception of flg22 triggers the rapid association of FLS2 with another LRR-RLK, BRI1-ASSOCIATED RECEPTOR KINASE1 (BAK1) (Chinchilla et al., 2007; Heese et al., 2007). A receptor-like cytoplasmic kinase, BOTRYTIS-INDUCED KINASE1 (BIK1), associates with the FLS2 receptor complex and directly phosphorylates the NADPH oxidase RbohD, resulting in a calcium burst and reactive oxygen species production (Lu et al., 2010; Zhang et al., 2010; Kadota et al., 2014; Li et al., 2014). In addition, flagellin perception triggers the activation of mitogen-activated protein kinases (MAPKs), induction of immune-responsive genes, callose deposition to reinforce the cell wall, and immunity to a broad spectrum of pathogens (Jones and Dangl, 2006; Dodds and Rathjen, 2010; Tang et al., 2017).

The immune responses must be tightly controlled to ensure optimal magnitude and appropriate duration. Direct ubiquitination of FLS2 by two closely related U-box E3 ubiquitin ligases, PUB12 and PUB13, leads to the attenuation of immune signaling (Lu et al., 2011). A BAK1-interacting kinase, BAK1-INTERACTING RECEPTOR-LIKE KINASE2 (BIR2), negatively regulates PTI by preventing BAK1-receptor complex formation in the absence of PAMPs. Upon flg22 perception, BIR2 is released from BAK1 and enables the association of BAK1 with FLS2 (Halter et al., 2014). PTI also can be fine-tuned by the rapid release of small peptides like rapid alkalinization factor23, which binds to its receptor FERONIA to inhibit immunity. Otherwise, FERONIA serves as a scaffold to promote the complex assembly of the immune receptor and its coreceptor BAK1 (Stegmann et al., 2017). In addition, protein phosphatase2A (PP2A) associates with BAK1 and modulates its phosphostatus, thereby negatively regulating plant innate immunity (Segonzac et al., 2014). Immune signaling also can be regulated by controlling the turnover of BIK1. Nonactivated BIK1 is ubiquitinated by PUB25 and PUB26 for degradation (Wang et al., 2018). The heterotrimeric G proteins inhibit the E3 ligase activity of PUB25/26, thereby stabilizing BIK1, whereas CALCIUM-DEPENDENT PROTEIN KINASE28 specifically phosphorylates PUB25/26 to boost their activity and promote BIK1 degradation (Monaghan et al., 2014; Liang et al., 2016; Wang et al., 2018). FLS2-mediated immunity also can be positively regulated by the transcriptional control of *FLS2* through the transcription factors ETHYLENE INSENSITIVE3 (EIN3) and EIN3-LIKE1 (Boutrot et al., 2010). Overall, relative to the growing number of regulatory mechanisms functioning at the protein level, much less is known about those working through transcriptional regulation of the components of the immune receptor complex.

Immunity varies with age. Age-dependent immune responses have been observed in plants (Zhao et al., 2009; Saur et al., 2016).

[1]These authors contributed equally to this work.
[2]Address correspondence to [dplu@sjziam.ac.cn].
The author responsible for distribution of materials integral to the findings presented in this article in accordance with the policy described in the Instructions for Authors (www.plantcell.org) is: Dongping Lu (dplu@sjziam.ac.cn).
www.plantcell.org/cgi/doi/10.1105/tpc.18.00297

IN A NUTSHELL

Background: Plants and animals largely rely on innate immunity to protect themselves from pathogen infections. Recognition of pathogen-associated molecular patterns (PAMPs) by plant pattern recognition receptors (PRRs) initiates PAMP-triggered immunity in plants. FLAGELLIN-SENSING2 (FLS2) is a well-known PRR that recognizes bacterial flagellin. Immunity varies with age. The human immune system in early life undergoes rapid, radical changes and displays large differences from that of adults. As in humans, age-dependent immune responses have also been observed in plants. However, little is known about the ontogeny of plant innate immunity during seedling development.

Question: We wanted to know whether FLS2-mediated immunity involves an ontogenetic process. If so, what are the mechanisms that regulate the ontogeny of plant innate immunity.

Findings: We found that FLS2-mediated immunity during seedling development involves an ontogenetic process. The transcription of *FLS2* controls the ontogeny of FLS2-mediated immunity. Importantly, the *Arabidopsis thaliana* microRNA miR172b regulates the transcription of *FLS2* through TARGET OF EAT1 (TOE1) and TOE2, two targets of miR172b. These two transcription factors (TOE1 and TOE2) directly bind to the *FLS2* promoter and inhibit its activity. The level of miR172b is low in the very early stage of seedling development. Consequently, the TOE1/2 protein levels are high in the same stage. Furthermore, miR172b abundance increases during seedling development, while the TOE1/2 protein levels decrease with time, which results in increased *FLS2* transcription and the ontogeny of FLS2-mediated immunity.

Next steps: We show that miR172b regulates the transcription of *FLS2* through TOE1 and TOE2, which governs the ontogeny of plant innate immunity. This finding prompts us to investigate additional mechanisms and components that regulate the ontogeny of plant innate immunity.

For example, the immune responses mediated by RECEPTOR-LIKE PROTEIN REQUIRED FOR CSP22 RESPONSIVENESS (NbCSPR) were greater in 6-week-old than in 4-week-old *Nicotiana benthamiana* plants (Saur et al., 2016). However, to date, little is known about plant innate immunity in the course of seedling development. Here, we show that the microRNA miR172b regulates the transcription of *FLS2* through TARGET OF EAT1 (TOE1) and TOE2, which governs the ontogeny of plant innate immunity.

RESULTS

Transcription of *FLS2* Governs the Ontogeny of flg22-Triggered Immunity during Seedling Development

To characterize innate immunity during seedling development, we analyzed flg22-triggered immune responses in Arabidopsis (*Arabidopsis thaliana*) Col-0 plants 2, 3, and 6 d after germination (Supplemental Figure 1). Flg22-induced callose deposition, MAPK activation, and expression of immune-responsive genes, such as *At1g51890*, *PEROXIDASE4* (*PER4*) (Malinovsky et al., 2014), and *FLG22-INDUCED RECEPTOR-LIKE KINASE1* (*FRK1*), all were increased progressively during the first week after germination (Figures 1A–1C). This suggests that the flg22-triggered immunity in the course of seedling development may involve an ontogenetic process.

We then monitored MAPK activation in *fls2* plants induced by a PP2A inhibitor, cantharidin, which removes the negative regulation of BAK1 imposed by PP2A (Segonzac et al., 2014). During the first week after germination, MAPK activation induced by cantharidin in *fls2* seedlings was not increased with time (Figure 2A), suggesting that the ontogeny of immunity during seedling development may not be controlled by the MAPK cascade or BAK1 but may be governed by other upstream components in the PTI signaling pathway. Notably, the expression of *FLS2* increases significantly during seedling development (Figure 2B). Furthermore, transgenic plants with the *FLS2* promoter (*ProFLS2*) fused to a reporter gene encoding GUS showed increased GUS activity between 2 and 6 d (Figure 2C). These results suggest that the ontogeny of flg22-triggered immunity during seedling development may be controlled through the transcriptional regulation of *FLS2*. To confirm this inference, we monitored flg22-induced MAPK activation in *Pro35S:FLS2-YFP-HA/fls2* transgenic plants (Shi et al., 2013) and found that MAPK activation did not increase during seedling development when *FLS2* was driven by a constitutive promoter (Figure 2D).

TOE1/2 Suppress *FLS2* Promoter Activity

We hypothesized that the transcriptional activation of *FLS2* in the course of seedling development could be due to the absence of transcriptional activators at 2 dpg that are progressively upregulated or to the presence of potential transcriptional suppressors of *FLS2* at 2 dpg that are downregulated as plants grow. It has been found that EIN3 serves as a transcriptional activator of *FLS2* (Boutrot et al., 2010). Therefore, we focused on screening transcriptional suppressors of *FLS2*. We performed RNA sequencing (RNA-seq) to identify downregulated transcription factor genes using RNA isolated from 2- and 6-d-old seedlings (Supplemental Figure 2A). We found that the expression of *EIN3* was increased during seedling development (Supplemental Figures 2B and 2C). Importantly, a total of 135 transcription factor genes were downregulated in the course of seedling development (Supplemental Figures 2D and 2E, Supplemental Data Set 1). Meanwhile, two brassinosteroid (BR)-repressed genes are expressed at lower levels in 2-d-old than in 6-d-old plants, and a cytokinin (CK)-responsive gene, *ARABIDOPSIS RESPONSE REGULATOR3* (*ARR3*), is expressed at a higher level in 2-d-old

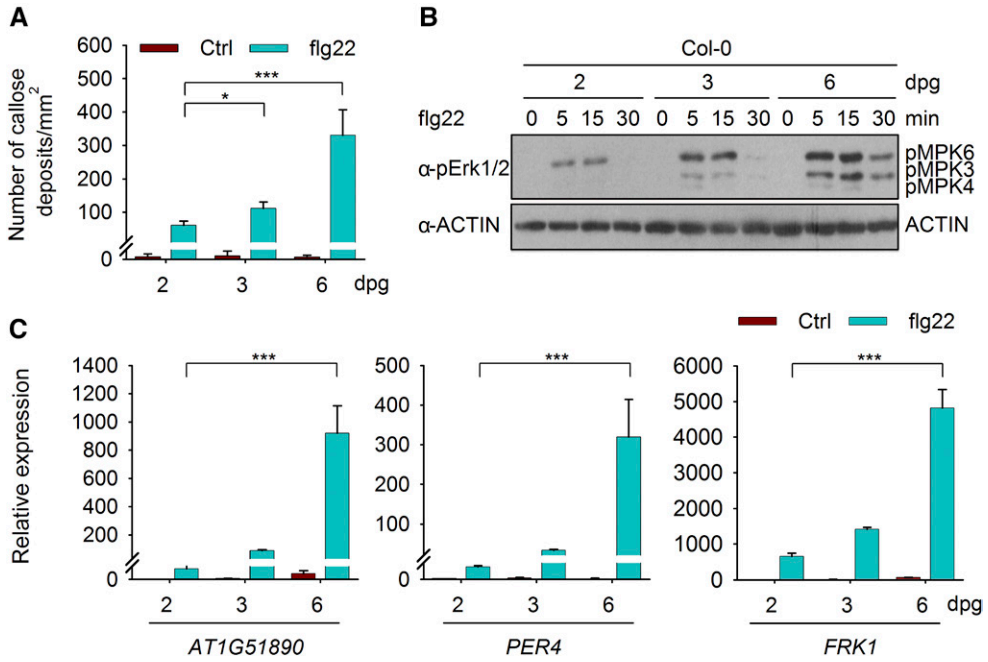

Figure 1. Flg22-Triggered Immunity Was Increased during Seedling Development.

(A) Flg22-induced callose deposition. Col-0 seedlings at the indicated ages (days post germination [dpg]) were treated with 1 μM flg22 for 12 h. Data are shown as means ± SD (n = 6 leaves from different seedlings). Statistical significance compared with 2-d-old plants was assessed using one-way ANOVA followed by Student-Newman-Keuls tests: *, $P < 0.05$ and ***, $P < 0.001$. Three independent replicates were performed, and similar results were obtained.

(B) Flg22-triggered MAPK activation. Col-0 seedlings were treated with 100 nM flg22. MAPK activation was detected by immunoblotting with anti-pErk1/2 antibodies. ACTIN was detected as a loading control. This experiment was repeated three times with similar results.

(C) Flg22-induced gene induction. Col-0 seedlings were treated with 100 nM flg22 for 3 h. The expression of *At1g51890*, *PER4*, and *FRK1* was analyzed by RT-qPCR. Expression levels were normalized to those of *GAPC*. Values are means ± SD (n = 3). Statistical significance compared with 2-d-old plants was assessed using one-way ANOVA followed by Student-Newman-Keuls tests: ***, $P < 0.001$. Three independent replicates were performed, and similar results were obtained.

than in 6-d-old plants, suggesting that BR and CK signaling may be more active during the early stage of plant growth after germination (Supplemental Figures 2B and 2C).

To examine which transcription factors could suppress *FLS2* promoter activity, we performed a leaf protoplast cell-based screen by transiently expressing either the *firefly luciferase* (*LUC*) reporter gene or the *GFP* gene driven by the *FLS2* promoter along with one of the candidate transcription factor genes (Supplemental Figure 3). To validate the functionality of this screening system, we first transiently expressed *EIN3-HA* together with *ProFLS2*:*LUC* or *ProFLS2*:*GFP*. Consistent with the previous report (Boutrot et al., 2010), EIN3 enhanced *ProFLS2* activity in protoplasts (Supplemental Figures 4A and 4B). We then screened more than 100 of the 135 transcription factors identified above, using this protoplast transient expression system, and found that TOE1 and its closest homolog, TOE2, significantly suppressed *ProFLS2* activity when they were expressed in protoplasts (Supplemental Figures 5 and 6A–6C). TOE1 and TOE2 belong to a subfamily of AP2-like transcription factors (Aukerman and Sakai, 2003; Schmid et al., 2003). However, AP2 did not suppress *ProFLS2* activity (Supplemental Figure 6D). Moreover, the suppression of *ProFLS2* activity by TOE1/2 was dose dependent (Figures 3A and 3B).

To further confirm these results, we deleted the nuclear localization signals (NLSs) of TOE1/2 and generated the TOE1/2$^{\triangle NLS}$ mutants (Jofuku et al., 1994) (Figure 3C). Then, we transiently expressed TOE1/2-GFP or TOE1/2$^{\triangle NLS}$-GFP together with WRKY48-RFP, a nucleus-localized protein (Xing et al., 2008), in Arabidopsis protoplasts. We found that the fluorescence patterns of TOE1/2-GFP overlapped with that of RFP-tagged WRKY48 while those of TOE1/2$^{\triangle NLS}$-GFP did not, although a significant proportion of the mutant proteins could be localized predominantly to nuclear foci. Consequently, TOE1/2$^{\triangle NLS}$ could not suppress *ProFLS2* activity (Figures 3D–3G).

To examine whether TOE1 could regulate other PRRs, like the elongation factor EF-Tu receptor (EFR) (Zipfel et al., 2006), we transiently expressed *TOE1-HA* together with *ProEFR*:*GFP* (*GFP* gene driven by the *EFR* promoter) in Arabidopsis protoplasts. We found that TOE1 could suppress *ProEFR* activity (Supplemental Figure 7), suggesting that TOE1 also may regulate EFR-mediated immunity.

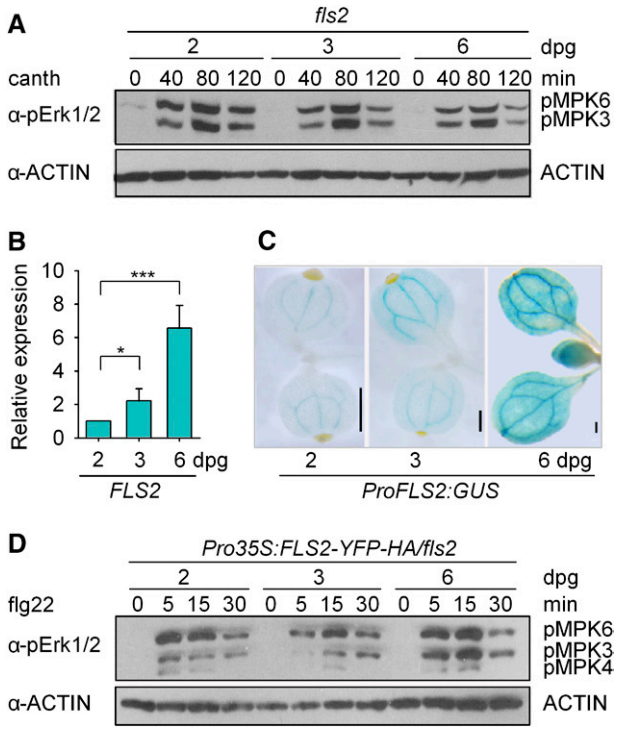

Figure 2. Transcription of *FLS2* Controls the Ontogeny of flg22-Triggered Immunity during Seedling Development.

(A) MAPK activation induced by cantharidin is not increased during seedling development. Two-, 3-, or 6-d-old *fls2* seedlings were treated with 80 μM cantharidin (canth) for the indicated times. ACTIN was examined as a loading control. This experiment was repeated three times with similar results.

(B) Measurement of *FLS2* mRNA levels by RT-qPCR. The levels were normalized to those of *GAPC*. Values are means ± SD of three biological replicates using independent pools of seedlings grown under the same conditions. Statistical significance compared with 2-d-old Col-0 plants was assessed using one-way ANOVA followed by Student-Newman-Keuls tests: *$P < 0.05$ and ***$P < 0.001$.

(C) GUS activity analysis for *ProFLS2*:*GUS* transgenic plants. Bars = 250 μm.

(D) Flg22-triggered MAPK activation in *Pro35S*:*FLS2-YFP-HA/fls2* transgenic plants. Seedlings were treated with 100 nM flg22. ACTIN was detected as a loading control. This experiment was repeated three times with similar results.

We then performed chromatin immunoprecipitation (ChIP) assays using transiently expressed TOE1-HA in Arabidopsis protoplasts. Region F of the *FLS2* promoter was enriched in TOE1-HA-immunoprecipitated chromatin at a markedly higher level than other regions (Figures 4A and 4B). The association between TOE1/2 and region F was confirmed by ChIP assays using *ProTOE1*:*TOE1-HA* and *ProTOE2*:*TOE2-HA* transgenic plants at 2 dpg, as *TOE1* and *TOE2* are expressed at relatively high levels at this developmental stage (Figure 4C, Supplemental Data Set 1).

To determine whether TOE1/2 is capable of binding directly to the *FLS2* promoter, we conducted electrophoretic mobility shift assays (EMSAs) with purified recombinant SUMO-TOE1/2. Region F of the *FLS2* promoter was divided into four fragments (F-1 to F-4) with some overlap (Figure 5A). The SUMO-TOE1 fusion protein was only able to bind to the DNA probes corresponding to F-2. The addition of an excess of unlabeled F-2 probes effectively reduced the binding of SUMO-TOE1 to the biotin-labeled F-2 probes. Similar results also were observed for SUMO-TOE2 (Figures 5B and 5C).

It was shown recently that TOE1 can associate with AT-rich elements (ATREs), TOE binding site (TBS)-like motifs, and other unknown DNA sequences in the promoter of *FLOWERING LOCUS T* (*FT*) (Zhai et al., 2015; Zhang et al., 2015). Sequence analysis failed to identify any ATRE, TBS, or TBS-like motif in the F-2 fragment of the *FLS2* promoter. However, F-2 contains three motifs (Motifs 1–3) rich in A/T (Figure 5D). To determine whether these motifs can bind to TOE1, we performed EMSAs with each motif repeated four times as a probe. The results showed that only Motif 1 could bind to TOE1, and a mutated form of Motif 1, Mu1, could not compete with wild-type Motif 1 for binding to TOE1 (Figure 5E, Supplemental Figure 8). Motif 1 (ATCTATATC), therefore, is named as TOE binding site in the *FLS2* promoter (TBSF). Similarly, TOE2 also was able to bind to the TBSF motif (Figure 5E). This result was further confirmed when only TBSF was mutated in F-2 (Mu4). As demonstrated in Figure 5F, Mu4 failed to compete with wild-type F-2 for binding to SUMO-TOE1. EMSA competition assays also were performed with the previously identified TBS-like motif from the *ProFT* directly as a competitor (Zhai et al., 2015). The results showed that the addition of an excess of unlabeled probes of TBS-like motifs (repeated four times as a probe) effectively reduced the binding of SUMO-TOE1 to the biotin-labeled TBSF probes (repeated four times as a probe) (Figure 5G). Moreover, a region from the *ProFT* containing a TBS-like motif can successfully compete with F-2 from the *ProFLS2* for binding to SUMO-TOE1 (Supplemental Figure 9).

TOE1/2 Negatively Regulate FLS2-Mediated Immunity during Seedling Development

TOE1/2 can suppress *FLS2* promoter activity, so we tested the expression of *FLS2* in 2-d-old *toe1 toe2* mutant plants. As expected, the level of *FLS2* transcripts in 2-d-old *toe1 toe2* plants was remarkably higher than that of wild-type plants (Figure 6A). Flg22-induced MAPK activation in 2-d-old *toe1 toe2* plants was much stronger than that in wild-type plants (Figure 6B). Moreover, the induction of the immune-responsive genes, *At1g51890*, *PER4* (Malinovsky et al., 2014), and *FRK1*, in 2-d-old *toe1 toe2* mutant plants was much greater than that in wild-type plants (Figure 6C).

Then, we examined the sensitivity of *toe1-2*, *toe2-1*, and *toe1 toe2* mutant plants (Aukerman and Sakai, 2003; Wu et al., 2009) to flg22 by seedling growth inhibition assays. Because the seedling growth inhibition assay involves a relatively long duration of flg22 treatment, we transferred 1-d-old plants to medium containing flg22. After 5 d of growth, *toe1-2*, *toe2-1*, and *toe1 toe2* plants showed enhanced sensitivity to flg22 compared with wild-type plants; the phenotype was stronger in *toe1 toe2* than in either single mutant (Figure 6D), suggesting that *TOE1* and

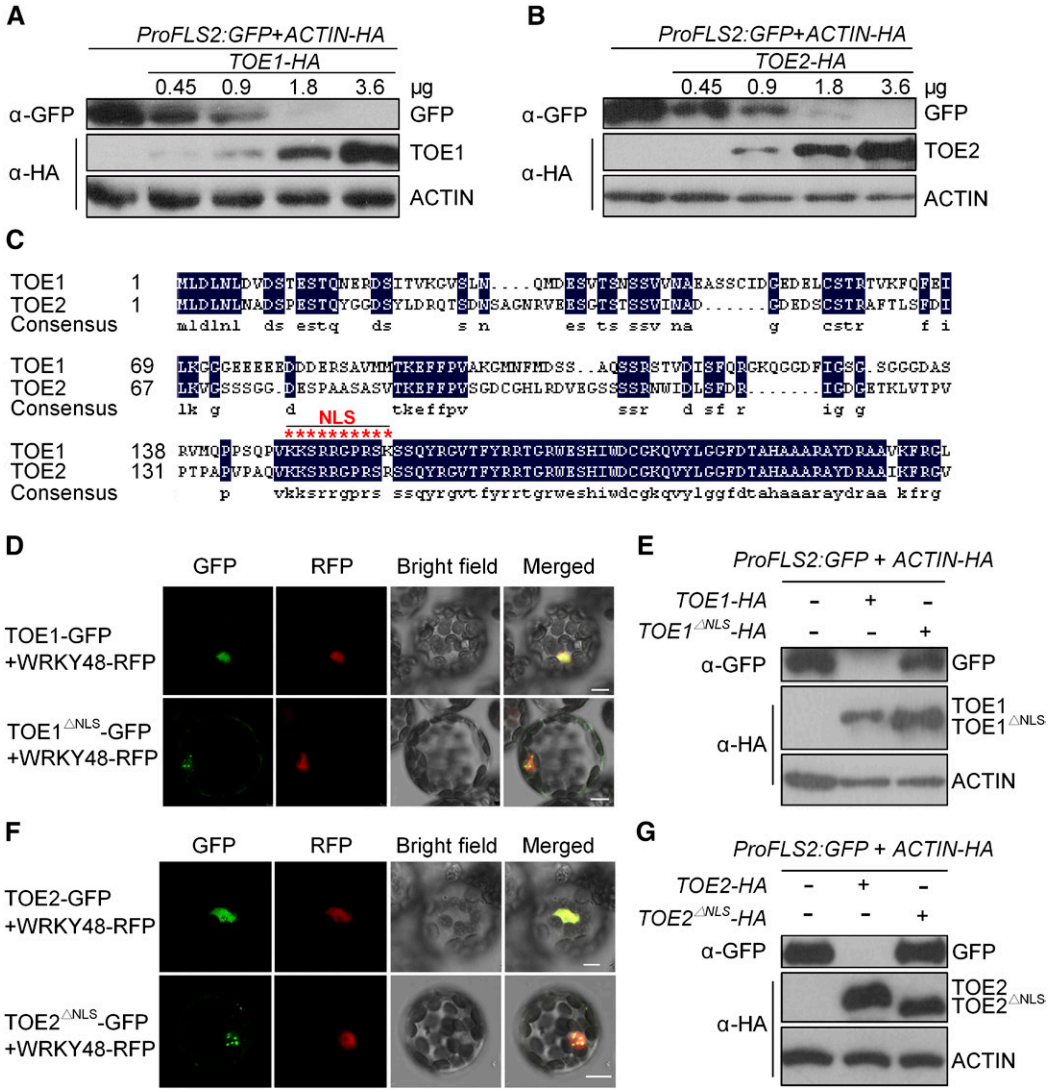

Figure 3. TOE1/2 Suppress *FLS2* Promoter Activity.

(A) and **(B)** The suppression of *ProFLS2* activity by TOE1 **(A)** or TOE2 **(B)**. *TOE1/2-HA* was coexpressed with *ProFLS2*:*GFP* in protoplasts. *ACTIN-HA* was coexpressed as an internal transfection control. The expression of *ProFLS2*:*GFP* was detected by immunoblotting. The experiments were repeated three times with similar results.

(C) Alignment of the N termini of TOE1 and TOE2. The NLS is highlighted with red asterisks.

(D) and **(F)** Subcellular localization of TOE1/2 NLS deletion mutants, TOE1/2$^{\triangle NLS}$. *TOE1/2-GFP* or *TOE1/2*$^{\triangle NLS}$*-GFP* was coexpressed with *WRKY48-RFP* in protoplasts. The protoplasts then were subjected to laser confocal imaging. Bars = 7.5 μm.

(E) and **(G)** TOE1/2$^{\triangle NLS}$ failed to suppress *FLS2* promoter activity. These experiments were repeated three times with similar results.

TOE2 have overlapping functions in regulating immunity. However, in the absence of flg22, there was no obvious difference among these plants during seedling development (Figure 6D). Moreover, *Pro35S*:*FLS2-YFP-HA/fls2* plants were phenotypically indistinguishable from *fls2* and wild-type plants when grown on one-half-strength Murashige and Skoog (1/2 MS) medium or in soil, and the difference among these plants was detected only in the presence of flg22 (Supplemental Figures 10A and 10B).

We also performed pathogen infection assays with 2-d-old *toe1 toe2* mutant and wild-type plants. *toe1 toe2* plants were more resistant than wild-type plants to *Pseudomonas syringae* pv *tomato* (*Pst*) DC3000 (Figure 6E). Additionally, when 2-d-old plants were treated with flg22 for 12 h, the induction of callose deposition by flg22 was stronger in *toe1 toe2* mutant plants than in wild-type plants (Figure 6F). These results suggest that the flg22-triggered immune responses in *toe1 toe2* plants are much stronger than those in wild-type plants and that TOE1/2 negatively regulate FLS2-mediated immunity during seedling development.

TOE1 and *TOE2* are targets of miR172 (Aukerman and Sakai, 2003; Schwab et al., 2005; Jung et al., 2007). It has been found

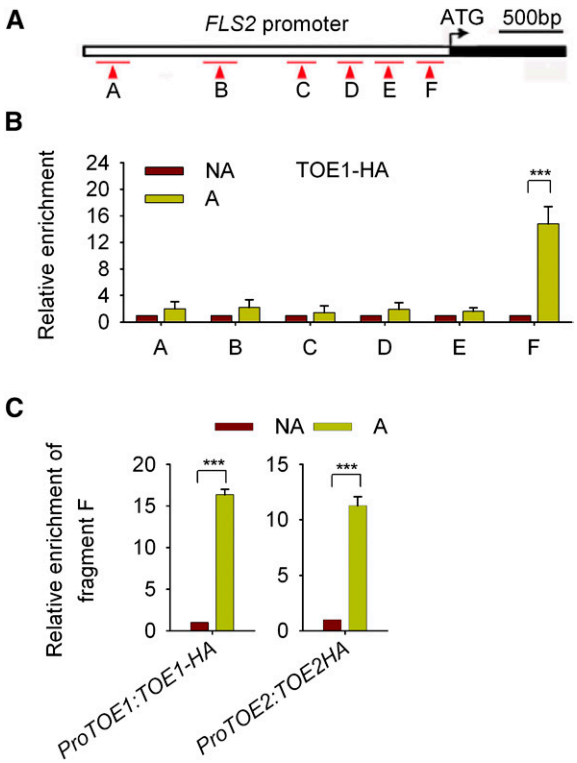

Figure 4. TOE1/2 Are Associated with Region F of the *FLS2* Promoter.

(A) The partial structure of the *FLS2* gene and regions amplified by ChIP-PCR.

(B) Enrichment of the indicated TOE1-associated DNA regions in protoplasts expressing TOE1-HA as determined by ChIP-PCR. *TOE1-HA* was transfected in protoplasts. Chromatin from protoplasts expressing TOE1-HA was immunoprecipitated with anti-HA antibodies, enrichment levels were normalized to those of protoplasts transfected with empty vectors, and no-antibody (NA) immunoprecipitates served as a control. Values are means ± SD of three biological replicates. Statistical significance compared with the NA control was determined by Student's *t* tests: ***P < 0.001.

(C) Enrichment of the F region DNA of the *FLS2* promoter in *ProTOE1*:*TOE1-HA* and *ProTOE2*:*TOE2-HA* transgenic plants. Chromatin from 2-d-old *ProTOE1/2*:*TOE1/2-HA* transgenic seedlings was immunoprecipitated with anti-HA antibodies, enrichment levels were normalized to those of Col-0 seedlings, and NA immunoprecipitates served as a control. Values are means ± SD ($n = 3$). Statistical significance compared with the NA control was determined by Student's *t* tests: ***P < 0.001. Three independent replicates were performed, and similar results were obtained.

that the expression of *miR172* was regulated temporally, and *miR172* abundance was increased progressively as plants grew until flowering, which leads to a gradual reduction in *TOE1/2* transcript levels (Aukerman and Sakai, 2003; Jung et al., 2007; Wu et al., 2009). Consistently, we found that *TOE1/2* transcript levels and the accumulation of TOE1/2 proteins decrease during seedling development (Figures 7A–7C). Furthermore, the TOE1/2 protein levels in 2-d-old plants were decreased upon flg22 treatment (Figure 7D). Moreover, levels of *TOE1/2* transcripts and TOE1/2 proteins also decreased upon flg22 treatment at adult plant growth stages (Supplemental Figure 11). These results suggest that the flg22-triggered immunity during seedling development is suppressed by TOE1/2 but that this suppression is gradually removed with time. Moreover, the repression of *FLS2* by TOE1/2 also could be relieved upon flg22 treatment.

In addition, we found that the transgenic plants with the *TOE1* promoter (*ProTOE1*) fused to a *GUS* reporter gene did not show decreased GUS activity between 2 and 6 d (Supplemental Figure 12) or in response to flg22 treatment (Supplemental Figure 13). These results suggest that the observed decrease of *TOE1* transcripts during seedling development, or upon flg22 treatment, is controlled mainly at the posttranscriptional level rather than the transcriptional level.

miR172b Positively Regulates FLS2-Mediated Immunity during Seedling Development

TOE1 and *TOE2* are targets of miR172 (Aukerman and Sakai, 2003; Schwab et al., 2005; Jung et al., 2007; Wu et al., 2009). Therefore, we tried to elucidate the role of miR172 in regulating plant innate immunity through TOE1/2. Consistently, the expression of *FLS2*, flg22-triggered seedling growth inhibition, resistance to *Pst* DC3000, flg22-induced callose deposition, and the induction of the immune-responsive genes in transgenic plants overexpressing *miR172b* (OE) during seedling development were very similar to the observations in *toe1 toe2* plants (Figures 8A–8D, Supplemental Figure 14).

Consistent with the previous report (Aukerman and Sakai, 2003), levels of pre-miR172b and mature miR172b increased during seedling development or upon flg22 treatment in 2-d-old and 8-week-old plants (Figures 8E and 8F, Supplemental Figures 15 and 16). In addition, we found that *ProFLS2* activity was higher in protoplasts isolated from *miR172b* OE plants than that in protoplasts from Col-0 plants (Figure 9A). Notably, the large increase of *FLS2* transcripts observed in the course of seedling development was significantly compromised in *MIM172* transgenic plants, a stable knockdown line of miR172 (Todesco et al., 2010), although the level of *FLS2* transcripts in 6-d-old *MIM172* plants was still higher than that in 2-d-old plants (Supplemental Figure 17). These results suggest that miR172 positively regulates the expression of *FLS2* during seedling development, but which also may be regulated by other factors.

To verify that the regulation of *ProFLS2* activity by miR172b is mediated through TOE1/2, we first expressed a miR172-resistant form of *TOE1* (*rTOE1*) (Chen, 2004) in Arabidopsis protoplasts together with *ProFLS2*:*GFP*. The results showed that rTOE1 accumulated at a higher level than TOE1, leading to a stronger suppression of *ProFLS2* activity (Figure 9B). Moreover, we measured the *TOE1/2* mRNA levels in *MIM172* transgenic plants (Todesco et al., 2010) and found that the downregulation of *TOE1* and *TOE2* between 2 and 6 dpg no longer occurred in *MIM172* transgenic plants (Figure 7B, Supplemental Figure 18).

Then, we examined the levels of *TOE1/2* transcripts and their cleavage products in *miR172b* OE and wild-type plants. We found that the cleavage products of both *TOE1* and *TOE2* increased in *miR172b* OE compared with wild-type plants. The *TOE2* mRNA level decreased substantially in *miR172b* OE, whereas the steady-state level of *TOE1* mRNA declined only

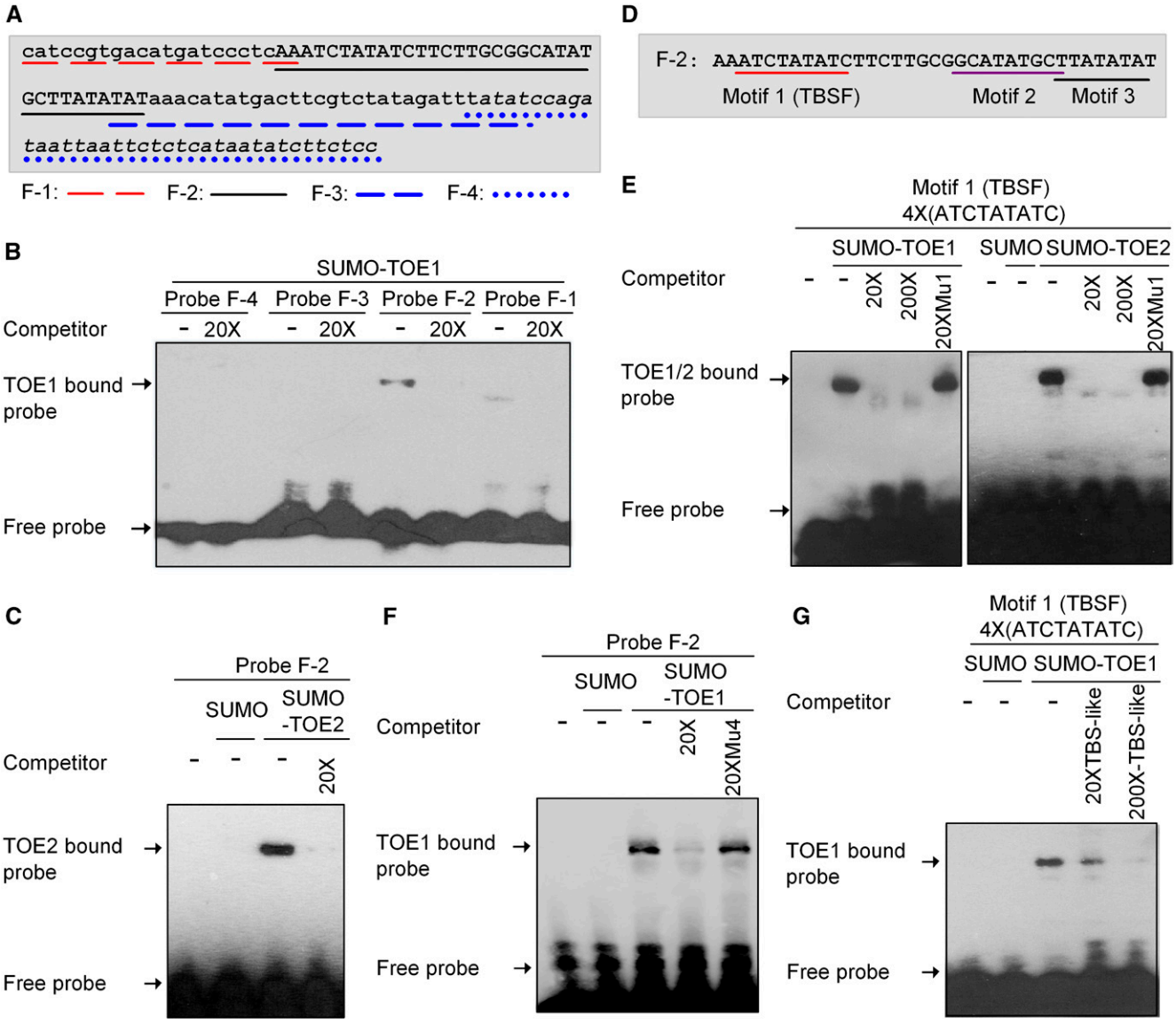

Figure 5. TOE1/2 Bind Directly to the *FLS2* Promoter.

(A) Region F of the *FLS2* promoter was divided into four fragments, F-1 to F-4.
(B) TOE1 binds to the F-2 DNA fragment. EMSA was performed with purified recombinant SUMO-TOE1 and each fragment (F-1 to F-4) as a probe. An excess of unlabeled DNA probes was added to compete with the biotin-labeled DNA probes. This experiment was repeated three times with similar results.
(C) TOE2 binds to the F-2 DNA fragment. EMSA was performed with purified recombinant SUMO-TOE2 and the F-2 DNA fragment as a probe. SUMO proteins were used as a negative control. This experiment was repeated three times with similar results.
(D) The F-2 fragment in the *FLS2* promoter contains three motifs rich in A/T (Motifs 1–3).
(E) Both TOE1 and TOE2 can bind to Motif 1. EMSA was performed with purified recombinant SUMO-TOE1/2 and Motif 1 (repeated four times) as a probe. An excess of unlabeled wild-type Motif 1 or its mutant (Mu1) DNA probes were added to compete with the biotin-labeled wild-type Motif 1 probes. Motif 1 was named as TBSF. These experiments were repeated three times with similar results.
(F) TOE1 binds to the TBSF motif in the F-2 DNA fragment. EMSA was performed with the F-2 DNA fragment as a probe. SUMO proteins were used as a negative control. Mu4 is a mutant form of the F-2 DNA fragment in which only TBSF was mutated. An excess of unlabeled wild-type F-2 or Mu4 DNA probes were added to compete with the biotin-labeled wild-type F-2 DNA probes. This experiment was repeated three times with similar results.
(G) EMSA competitions with purified recombinant SUMO-TOE1 and the TBS-like motif as a competitor. EMSA was performed with the TBSF motif (repeated four times) as a probe, and an excess of unlabeled probes of the TBS-like motif (from *ProFT*, repeated four times) was added. This experiment was repeated three times with similar results.

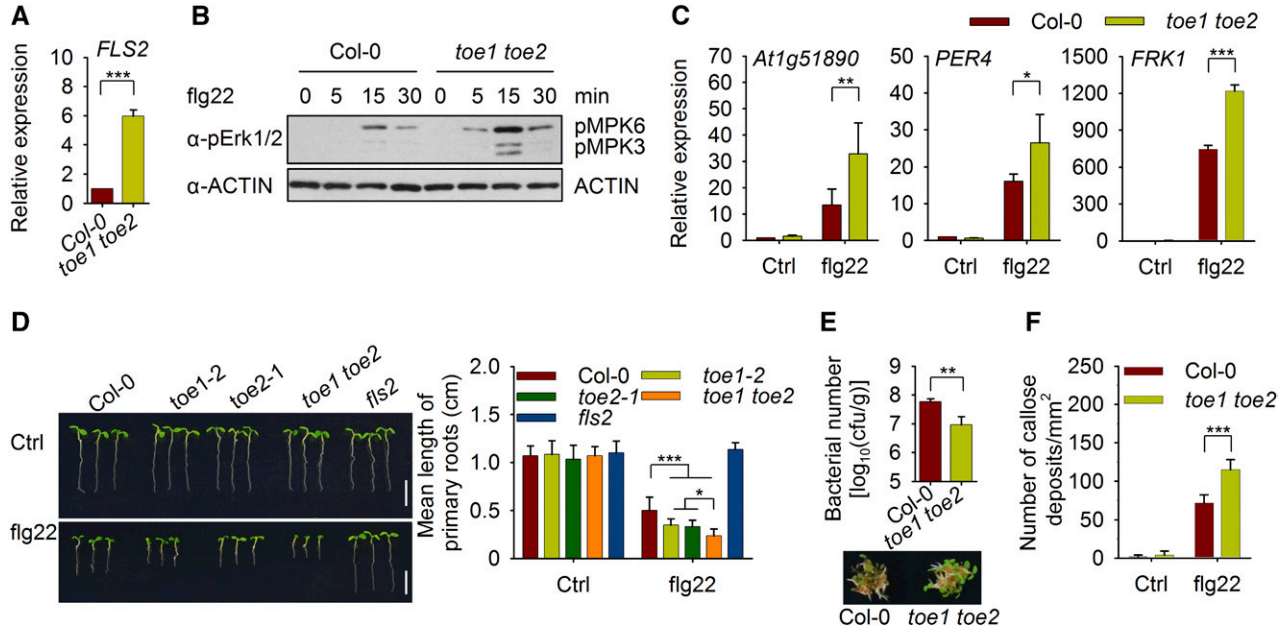

Figure 6. TOE1/2 Negatively Regulate FLS2-Mediated Immunity during Seedling Development.

(A) RT-qPCR analysis of *FLS2* expression in 2-d-old Col-0 and *toe1 toe2* seedlings. Expression levels were normalized to those of *GAPC*. Values are means ± SD of three biological replicates using independent pools of seedlings grown under the same conditions. Statistical significance compared with Col-0 was determined by Student's *t* tests: ***P < 0.001.

(B) Flg22-induced MAPK activation. Two-day-old Col-0 and *toe1 toe2* mutant plants were treated with 100 nM flg22 for the indicated times. MAPK activation was detected by immunoblotting with anti-pErk1/2 antibodies. ACTIN was detected as a loading control. This experiment was repeated three times with similar results.

(C) Flg22-induced gene induction in 2-d-old plants. Col-0 and *toe1 toe2* mutant seedlings were treated with 100 nM flg22 for 3 h. The expression of *At1g51890*, *PER4*, and *FRK1* was analyzed by RT-qPCR, and the expression levels were normalized to those of *GAPC*. Values are means ± SD of three biological replicates using independent pools of seedlings (45 seedlings per pool) grown under the same conditions. Statistical significance compared with Col-0 was assessed using one-way ANOVA followed by Student-Newman-Keuls tests: *P < 0.05; **, P < 0.01; and ***P < 0.001.

(D) Flg22-triggered seedling growth inhibition assay for Col-0, *toe1-2*, *toe2-1*, and *toe1 toe2* double mutant plants. One-day-old plants were transferred to medium containing 1 μM flg22 and grown for another 5 d. The quantification of growth inhibition is shown in the right panel. Values are means ± SD (n = 12 seedlings). Statistical significance was assessed using one-way ANOVA followed by Student-Newman-Keuls tests: *P < 0.05 and ***P < 0.001. Three independent replicates were performed, and similar results were obtained. Bars = 5 mm.

(E) Growth of *Pst* DC3000 on Col-0 and *toe1 toe2* plants. Two-day-old plants were inoculated with bacteria. Values are means ± SD of three biological replicates using independent seedling samples grown and inoculated under the same conditions. Statistical significance compared with Col-0 was determined by Student's *t* tests: **P < 0.01. Representative photographs of Col-0 and *toe1 toe2* seedlings infected with *Pst* DC3000 are shown in the lower panel. cfu, colony-forming units.

(F) Flg22-induced callose deposition in Col-0 and *toe1 toe2* plants. Two-day-old plants were treated with 1 μM flg22 for 12 h, and the number of callose deposits was counted using ImageJ. Values are means ± SD (n = 6 leaves from different seedlings). Statistical significance compared with Col-0 was assessed using one-way ANOVA followed by Student-Newman-Keuls tests: ***P < 0.001. Three independent replicates were performed, and similar results were obtained.

slightly (Supplemental Figures 19A and 19B), suggesting that, in *miR172b* OE plants, the steady-state level of at least *TOE1* transcripts might be modulated by feedback regulation, as reported previously (Schwab et al., 2005). Furthermore, TOE1 proteins were barely detected in *ProTOE1*:*TOE1-HA*/*miR172b* OE plants (Supplemental Figure 19C). These results confirmed that both *TOE1* and *TOE2* were downregulated in *miR172b* OE plants.

DISCUSSION

It has been reported that age affects immune responses in plants. The immunity mediated by NbCSPR was greater in 6-week-old than in 4-week-old *N. benthamiana* plants, which may be related to *NbCSPR* upregulation in 6-week-old relative to 4-week-old plants (Saur et al., 2016). In another report, the progressively enhanced rice resistance to *Xanthomonas oryzae* pv *oryzae* during plant growth from seedling stage to adult stage could be the consequence of the gradually increased expression of the LRR-RLK-type resistance genes *Xa3*/*Xa26* and *Xa21* (Zhao et al., 2009). Here, we found that Arabidopsis *FLS2* transcription increases progressively during seedling development, which regulates the ontogeny of plant innate immunity. Hence, transcriptional regulation of the immune receptor or related genes plays an important role in regulating age-dependent

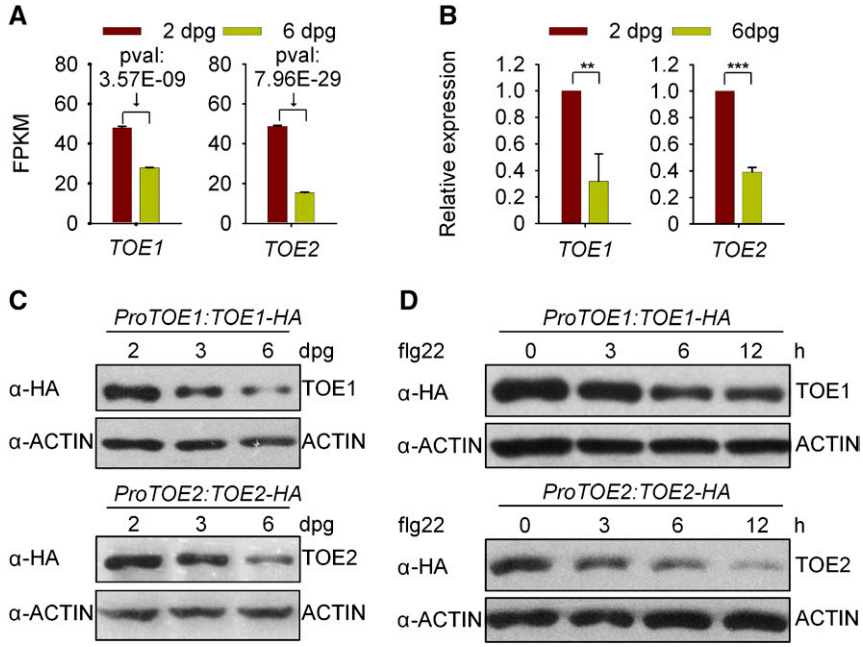

Figure 7. Expression Analysis of *TOE1* and *TOE2*.

(A) The fragments per kilobase of transcript sequence per million base pairs sequenced (FPKM) of *TOE1/2* during seedling development as determined by RNA-seq analysis. Values are means ± SD of two biological replicates. pval indicates the P value, which was adjusted using the Benjamini and Hochberg approach.

(B) Measurement of *TOE1/2* transcript levels during seedling development by RT-qPCR. The transcript levels were normalized to those of *GAPC*. Values are means ± SD of three biological replicates using independent pools of seedlings grown under the same conditions. Statistical significance compared with 2-d-old Col-0 was determined by Student's *t* tests: **P < 0.01 and ***P < 0.001.

(C) Immunoblotting analysis of TOE1/2 protein accumulation during seedling development. Total proteins were isolated from 2-, 3-, or 6-d-old *ProTOE1:TOE1-HA* or *ProTOE2:TOE2-HA* transgenic seedlings. ACTIN was examined as a loading control. These experiments were repeated three times with similar results.

(D) TOE1/2 protein levels were decreased upon flg22 treatment. Two-day-old transgenic seedlings were treated with 1 μM flg22 for the indicated times. These experiments were repeated three times with similar results.

immunity. The transcription of *FLS2* is regulated by *miR172b* through TOE1/2 that bind directly to the *FLS2* promoter and suppress its expression (Figure 10). However, the transcription factors modulating the expression of *NbCSPR* and resistance genes such as *Xa3*/*Xa26* and *Xa21* remain to be determined.

In this work, we found that TOE1/2 can bind directly to the TBSF motif in the *FLS2* promoter and inhibit its activity, although in vitro DNA affinity purification sequencing data do not provide evidence for the binding of TOE1/2 to this region in the *FLS2* promoter (O'Malley et al., 2016). In addition to TBSF, other TOE1 binding sites have been identified in the *FT* promoter. With its cofactor JASMONATE-ZIM DOMAIN1, TOE1 binds to a TBS-like motif in the *FT* promoter (Zhai et al., 2015). TOE1 also could interact with CONSTANS (CO) and bind to an ATRE motif in the *FT* promoter near the CO binding site (Zhang et al., 2015). These results implied that different cofactors may affect the binding of TOE1 to various DNA sequences. However, whether there are cofactors involved in the binding of TOE1 to the *FLS2* promoter remains to be determined.

It has been reported that EIN3 also binds directly to the *FLS2* promoter and positively controls *FLS2* expression (Boutrot et al., 2010). Terrestrial seed plants start growth under the soil. Notably, EIN3 protein levels are increased in response to soil overlay (Zhong et al., 2014). Consistently, our results showed that the expression of *EIN3* was increased in the course of seedling development (Supplemental Figures 2B and 2C). Therefore, the transcription of *FLS2* is regulated not only by the repression of TOE1/2 but also most likely by the upregulation of EIN3 or other unidentified factors to control the innate immunity ontogeny.

The suppression of FLS2-mediated immune responses during seedling development may be the result of a tradeoff between development and immunity. We found that a number of BR-repressed genes are expressed at lower levels in 2-d-old than in 6-d-old plants, suggesting that BR signaling may be more active during the early stage of seedling development (Supplemental Figures 2B and 2C). However, in the absence of flg22, even *Pro35S:FLS2-YFP-HA/fls2* seedlings were phenotypically indistinguishable from *fls2* and wild-type seedlings (Supplemental Figure 10). It has been found that the interaction between BR and PTI signaling is unidirectional: activation of BR signaling results in impaired PTI responses in Arabidopsis but not vice versa (Albrecht et al., 2012; Belkhadir et al., 2012; Lozano-Durán

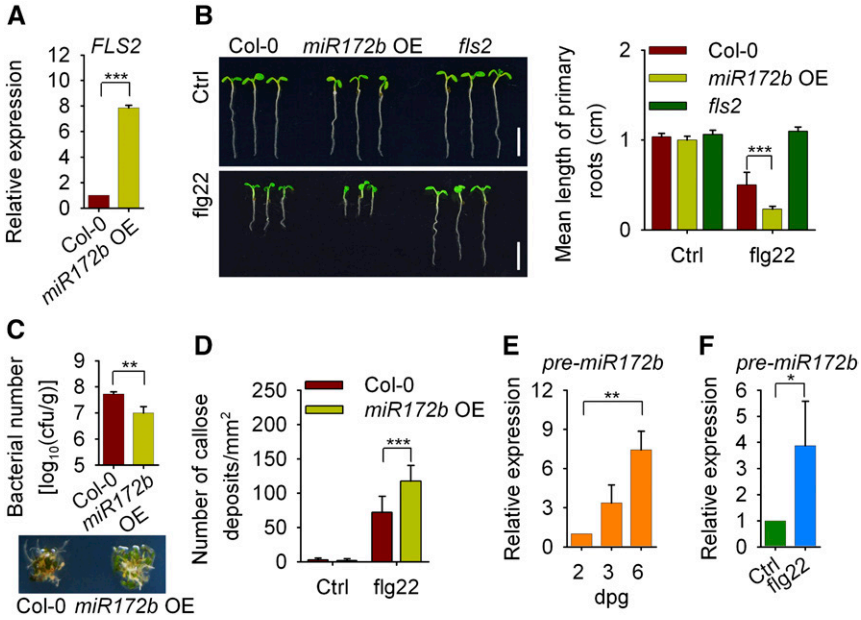

Figure 8. miR172b Positively Regulates FLS2-Mediated Immunity during Seedling Development.

(A) RT-qPCR analysis of *FLS2* expression in 2-d-old Col-0 and *miR172b* OE seedlings. Expression levels were normalized to those of *GAPC*. Values are means ± SD of three biological replicates using independent pools of seedlings (45 seedlings per pool) grown under the same conditions. Statistical significance compared with Col-0 was determined by Student's *t* tests: ***P < 0.001.

(B) Flg22-triggered seedling growth inhibition assay. One-day-old wild-type and *miR172b* OE plants were treated with 1 μM flg22 for 5 d. Quantification of growth inhibition is shown in the right panel. Values are means ± SD (*n* = 12 seedlings). Statistical significance compared with Col-0 was assessed using one-way ANOVA followed by Student-Newman-Keuls tests: ***P < 0.001. Three independent replicates were performed, and similar results were obtained. Bars = 5 mm.

(C) Growth of *Pst* DC3000 on Col-0 and *miR172b* OE plants. Two-day-old plants were inoculated with bacteria (OD_{600} = 5 × 10^{-4}). Bacterial growth was determined at 3 d post inoculation. Values are means ± SD of three biological replicates using independent seedling samples grown and inoculated under the same conditions. Statistical significance compared with Col-0 was determined by Student's *t* tests: **P < 0.01. Representative photographs of Col-0 and *miR172b* OE seedlings infected with *Pst* DC3000 are shown in the lower panel. cfu, colony-forming units.

(D) Flg22-induced callose deposition in Col-0 and *miR172b* OE plants. Two-day-old plants were treated with 1 μM flg22 for 12 h. Values are means ± SD (*n* = 6 leaves from different seedlings). Statistical significance compared with Col-0 was assessed using one-way ANOVA followed by Student-Newman-Keuls tests: ***P < 0.001. Three independent replicates were performed, and similar results were obtained.

(E) The expression of *miR172b* during seedling development. Total RNA was isolated from 2-, 3-, or 6-d-old seedlings. The pre-miR172b level was analyzed by RT-qPCR and was normalized to that of *GAPC*. Values are means ± SD of three biological replicates using independent pools of seedlings grown under the same conditions. Statistical significance compared with 2-d-old plants was assessed using one-way ANOVA followed by Student-Newman-Keuls tests: **P < 0.01.

(F) The expression of *miR172b* was induced by flg22 treatment. Two-day-old seedlings were treated with or without 100 nM flg22 for 3 h. Values are means ± SD of three biological replicates using independent pools of seedlings grown under the same conditions. Statistical significance compared with the control was determined by Student's *t* tests: *P < 0.05.

et al., 2013). Therefore, the active BR signaling in the course of seedling development may limit PTI responses. Additionally, the plant growth hormone CK modulates various aspects of plant growth (Naseem et al., 2015). We found that a CK-responsive gene, *ARR3*, is downregulated between 2 and 6 d, suggesting that CK signaling may be more active at the early stage of seedling development. It was reported that moderate activation of CK signaling could lead to the suppression of *FLS2* expression and, consequently, the impairment of immune responses like MAPK activation (Hann et al., 2014). However, whether CK signaling is related directly to miR172-mediated *FLS2* expression during seedling development remains to be investigated.

miR172 targets AP2-like transcription factors, such as *TOE1* and *TOE2*, and downregulates their expression by transcript cleavage or translation repression (Aukerman and Sakai, 2003; Schwab et al., 2005; Jung et al., 2007; Wu et al., 2009). It was found that the levels of miR172 and *TOE1* mRNA display a complementarity in tissues such as flowers, stems, and roots, suggesting that miR172 may regulate *TOE1* mainly through mRNA cleavage in these plant tissues (Jung et al., 2007). In addition, miR172 abundance increases as plants grow until flowering, while the levels of *TOE1/2* mRNA decrease progressively (Aukerman and Sakai, 2003; Jung et al., 2007). In *miR172* overexpression lines, the *TOE2* transcript level was reduced significantly but the steady-state levels of *TOE1* and *AP2* transcripts were not, whereas AP2 protein was decreased dramatically relative to wild-type plants. Therefore, it was suggested that miR172 may negatively regulate its targets through both mRNA cleavage

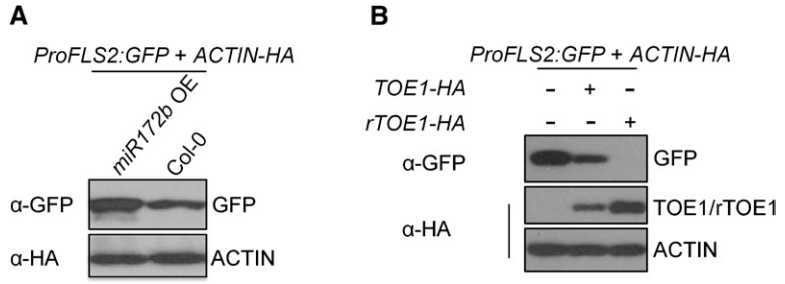

Figure 9. Regulation of *ProFLS2* Activity by miR172b Is Mediated through TOE1/2.

(A) *ProFLS2*:*GFP* was expressed in protoplasts isolated from Col-0 or *miR172b* OE plants.
(B) *ProFLS2*:*GFP* was coexpressed with *TOE1-HA* or *rTOE1-HA* in protoplasts.
For **(A)** and **(B)**, *ACTIN-HA* was coexpressed as an internal transfection control, and the expression of *ProFLS2*:*GFP* was detected by immunoblotting with anti-GFP antibodies.

and translational inhibition, and the steady-state transcript levels of miR172 targets also are modulated by feedback regulation (Aukerman and Sakai, 2003; Chen, 2004; Schwab et al., 2005; Jung et al., 2007). However, to date, the detection of TOE1/2 proteins in plants overexpressing miR172 has not been reported.

We found that miR172b abundance increases during seedling development, while the transcript and protein levels of *TOE1/2* decrease during the same period (Figures 7B, 7C, and 8E, Supplemental Figure 15). Furthermore, the reduction of *TOE1/2* transcript levels between 2 and 6 d was impaired in *MIM172* transgenic plants (Supplemental Figure 18). Therefore, miR172-guided transcript cleavage contributes to the downregulation of *TOE1* and *TOE2* during seedling development.

In *miR172* OE transgenic plants, both *TOE1* and *TOE2* are downregulated, but the underlying mechanisms appear to be more complicated. Consistent with the previous report (Schwab

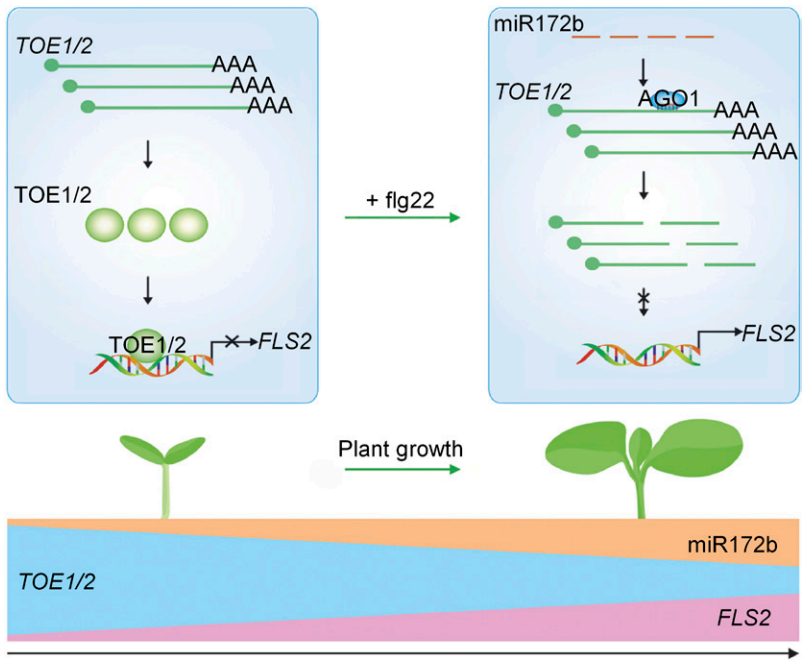

Figure 10. A Proposed Model of miR172b-Mediated Transcriptional Regulation of *FLS2* in Controlling the Ontogeny of Innate Immunity during Seedling Development.

TOE1 and TOE2 bind directly to the *FLS2* promoter and inhibit its activity. miR172b targets *TOE1* and *TOE2* and downregulates their expression. The level of miR172b is very low in the early stage of seedling development but increases over time, which results in decreased TOE1/2 protein accumulation and, consequently, the ontogeny of FLS2-mediated immunity. Additionally, the level of miR172b also is increased in plants challenged with flg22, leading to decreased TOE1/2 accumulation.

et al., 2005), *TOE2* mRNA decreased substantially in *miR172b* OE transgenic plants compared with wild-type plants, while the steady-state level of *TOE1* mRNA only declined slightly, although the cleavage products of both *TOE1* and *TOE2* were increased significantly in *miR172b* OE plants. Notably, we found that the TOE1 protein level was reduced dramatically in *miR172b* OE compared with wild-type plants (Supplemental Figure 19). Taken together, in *miR172b* OE plants, miR172b may downregulate *TOE2* primarily by mRNA cleavage. As for *TOE1*, feedback regulation may mask the effects of miR172b on *TOE1* mRNA level in *miR172b* OE plants, as has been proposed previously (Schwab et al., 2005; Jung et al., 2007), and *TOE1* may be regulated by miR172b through both transcript cleavage and translation repression in *miR172b* OE plants.

In this study, we demonstrate a function of the miR172-TOE1/2 module. miR172b-mediated transcriptional regulation of *FLS2* during seedling development controls the ontogeny of plant innate immunity (Figure 10). The role of the miR172-TOE1/2 module in controlling flowering timing has been studied extensively (Aukerman and Sakai, 2003; Jung et al., 2007; Wu et al., 2009). *miR172* abundance was very low in young seedlings but increased progressively as plants grew until flowering, which leads to a gradual reduction of TOE1/2 (Aukerman and Sakai, 2003; Jung et al., 2007; Wu et al., 2009). Once TOE1/2 proteins decrease below a critical threshold, flowering is triggered. It is likely that TOE1/2 prevents precocious flowering by repressing the expression of *FT*, one of the best characterized floral integrators (Kardailsky et al., 1999). TOE1 and TOE2 can bind directly to *FT* chromatin or interact with and repress CO, a positive transcriptional regulator of *FT* (Zhai et al., 2015; Zhang et al., 2015).

The temporal expression of *miR172* causes the temporal downregulation of *TOE1/2*, which presumably results in the increased transcription of *FLS2* beyond seedling development and throughout the life cycle. Furthermore, PAMP treatment also could cause the increased expression of *miR172* and the decreased expression of *TOE1/2* at both the seedling and adult plant stages (Figures 7D and 8F, Supplemental Figures 11 and 16). To ensure survival for any plant species, the most important thing is successful reproduction. Plants have evolved sophisticated mechanisms to coordinate their flowering timing in response to the ever-changing environment. Upon pathogen infections, plants either spend more resources for immunity, which is costly to development, or accelerate flowering to ensure that plants accomplish reproduction before succumbing to disease (Lyons et al., 2015). It has been found that infections by the bacteria *Pseudomonas syringae* and *Xanthomonas campestris* accelerate flowering in Arabidopsis (Korves and Bergelson, 2003). Therefore, the miR172-TOE1/2 module not only regulates the ontogeny of innate immunity and the flowering timing during the reproductive phase but also most likely serves as a major integrator to coordinate plant immunity, development, and flowering timing.

METHODS

Plant Material and Growth Conditions

For protoplast isolation and analysis of gene expression at adult plant growth stages, Arabidopsis (*Arabidopsis thaliana*) plants were grown in soil under 70 μE m^{-2} s^{-1} light (white fluorescent bulbs) with a 12-h photoperiod in a growth room at 22°C with 60% relative humidity for 30 d. The mutants *fls2*, *toe1-2* (SALK_069677), *toe2-1* (SALK_065370), and *toe1 toe2* and the transgenic plants *miR172b* OE, *Pro35S:FLS2-YFP-HA*/*fls2*, and *MIM172* were described previously (Shan et al., 2008; Wu et al., 2009; Todesco et al., 2010; Shi et al., 2013). Primers used for genotyping are listed in Supplemental Data Set 2. Seeds were surface sterilized with 50% (v/v) bleach for 5 min and washed at least four times with sterile water. Sterile seeds were germinated and grown on 1/2 MS plates or liquid 1/2 MS medium supplemented with 0.5% (w/v) sucrose. The plates were kept for 2 d in the dark at 4°C to break dormancy (stratification) and transferred thereafter to a growth room at 22°C with a 12-h photoperiod. When comparing plants at different dpg, samples were collected at the same time of day to avoid the effects of photoperiod on the expression of *TOE1/2* and other genes (Zhang et al., 2015).

Plasmid Construction, Generation of Transgenic Plants, and Crosses

Arabidopsis *TOE1*, *TOE2*, *AP2*, *EIN3*, and other transcription factor genes were amplified by PCR from Col-0 cDNA and introduced into a plant expression vector. *TOE1/2*$^{\triangle NLS}$ mutations were generated by overlap extension PCR as described (Xiao et al., 2007). For *ProFLS2:LUC*, *ProFLS2:GFP*, and *ProFLS2:GUS*, 2.7 kb of genomic DNA sequence upstream of the *FLS2* start codon was amplified and fused to *LUC*, *GFP*, or *GUS* in a plant expression vector or pCAMBIA1391 vector. Full-length *TOE1/2* was subcloned into a protein expression vector, pET28a-SUMO, using *Bam*HI and *Hind*III sites for subcloning *TOE1* or *Bam*HI and *Xho*I sites for subcloning *TOE2*. *TOE1/2* transgenic plants were generated in Col-0 by *Agrobacterium tumefaciens*-mediated transformation with *TOE1/2* fused to an *HA* tag in the pTF101 vector under the control of its native promoter (~2 kb upstream of its start codon). For *ProTOE1:GUS*, the *TOE1* promoter was fused to a GUS reporter gene in the pCAMBIA1391 vector. The *TOE1/2* promoter was amplified from Col-0 genomic DNA. All primers are listed in Supplemental Data Set 2. The *ProTOE1:TOE1-HA*/*miR172b* OE plants were generated by crossing *ProTOE1:TOE1-HA*/Col-0 into the *miR172b* OE plants.

RT-qPCR, Stem-Loop RT-PCR, and 5′ RACE

To collect RNA of young Arabidopsis seedlings, 0.02 g of 2-, 3-, or 6-d-old plants grown in liquid medium was treated with 100 nM flg22 for 3 h, and total RNA was isolated from whole seedlings. To collect RNA of older plants, rosette leaves from 8-week-old plants were infiltrated with 100 nM flg22 or water, then the samples were harvested at 3 h post infiltration and total RNA was isolated from infiltrated leaves using TRIzol (Invitrogen) according to the manufacturer's instructions. cDNA was synthesized in 20-μL reactions using 1 μg of DNase I-treated total RNA with a reverse transcription system (Invitrogen). Real-time PCR was performed on a Bio-Rad CFX-96 Real-Time PCR system using a SYBR Green RT-PCR kit (Takara). Expression levels were normalized to the expression of *GAPC*, a stably expressed reference gene.

Stem-loop-specific reverse transcription was performed as described previously (Chen et al., 2005; Kulcheski et al., 2010). The level of mature microRNA was normalized to that of snoR101. To map the 5′ ends of the cleavage products of *TOE1/2* transcripts, 5′ RACE was performed using the 5′-full RACE Kit (Takara). Primers are listed in Supplemental Table 1.

Callose Deposition

Plants were treated with 1 μM flg22 for 12 h, and then callose deposition was analyzed as described previously (Gómez-Gómez and Boller, 2000;

Lu et al., 2011). Callose deposits were counted using the analyze particles function of ImageJ 1.42q software (http://rsb.info.nih.gov/ij/). Six different leaves were analyzed for each genotype.

MAPK Assays

MAPK assays were performed using 0.015 g of 2-, 3-, or 6-d-old seedlings grown in liquid medium. Seedlings then were stimulated with 100 nM flg22 or 80 μM cantharidin (Sigma-Aldrich). Total proteins were isolated from whole seedlings. MAPK activation was monitored by immunoblotting with anti-pErk1/2 antibodies (Cell Signaling Technology). ACTIN was examined as a loading control by immunoblotting with anti-β-ACTIN antibodies (Cell Signal Pathway Research Tools Supplier).

GUS Staining

Histochemical staining for GUS activity was performed as described previously (Sun et al., 2009). Plant tissues were incubated in a solution (100 mM sodium phosphate [pH 7.0], 0.5 mM potassium ferrocyanide, 0.5 mM potassium ferricyanide, 1 mg/mL 5-bromo-4-chrolo-3-indolyl-β-D-glucuronide [Sigma-Aldrich], and 0.1% [v/v] Triton X-100) at 37°C in the dark for 6 h. The GUS-stained samples were dehydrated with 75% (v/v) ethanol three times and then subjected to imaging using a Leica laser scanning microscope.

Transcriptome Sequencing

Total RNA for transcriptome sequencing was extracted using TRIzol reagent (Invitrogen) according to the manufacturer's instructions. RNA concentrations were measured using a NanoDrop 2000 spectrophotometer (ND-2000, ThermoFisher Scientific). Library preparation, sequencing, and data analysis were performed by Novogene. Raw reads in FASTA format were first processed through in-house Perl scripts. At the same time, Q20, Q30, and GC content were calculated for the clean data. Then, the high-quality clean reads were aligned to the reference genome using TopHat v2.0.12. Next, HTSeq v0.6.1 (Trapnell et al., 2009) was used to count the number of fragments per kilobase of transcript sequence per million base pairs sequenced. Differential expression analysis of seedlings at 2 and 6 dpg for two biological replicates was performed using the DESeq R package (1.18.0). P values for differential expression were calculated using a model based on the negative binomial distribution and were adjusted using the Benjamini and Hochberg approach. Genes with $P < 0.05$ were defined as differentially expressed. The R package pheatmap was used to generate a clustered heat map for differentially expressed genes.

Transient Gene Expression in Protoplasts

Protoplast isolation and gene transient expression were performed as described (Yoo et al., 2007). Briefly, protoplasts were collected 12 h post transfection for promoter activity or gene expression assays. For reporter assays, *ProUBQ10*:*GUS* was cotransfected as an internal transfection control, and the promoter activity was calculated as the LUC/GUS ratio. Protein expression was detected by immunoblotting with anti-GFP, anti-FLAG, or anti-HA antibodies (Sigma-Aldrich).

Recombinant Protein Isolation and EMSA

Recombinant SUMO proteins and SUMO-TOE1/2 fusion proteins were purified from *Escherichia coli* by affinity chromatography using Ni^{2+}-affinity matrices (Qiagen) according to the manufacturer's instructions. For EMSAs, biotin-labeled DNA probes were prepared by annealing pairs of complementary oligonucleotides with their corresponding sequences. EMSAs were performed using a LightShift Chemiluminescent EMSA Kit (Thermo Scientific). Binding reactions contained 4 μL of protein extract, 2 μL of 10 pM probe, 2 μL of 10× binding buffer, 100 mM $MgCl_2$, 1 μL of 5% (v/v) glycerol, 1 μL of 1 μg/μL poly(dI-dC), and double-distilled water to a total volume of 20 μL. Each reaction was incubated at 25°C for 30 min. All probe sequences are listed in Supplemental Table 2.

ChIP Assays

For ChIP assays using transiently expressed TOE1 proteins, 5 mL of protoplasts was transfected with *TOE1-HA* or control plasmids and incubated for 8 h, and cells were collected for subsequent use. For ChIP assays using transgenic plants, 2-d-old *ProTOE1*:*TOE1-HA*, *ProTOE2*:*TOE2-HA*, and wild-type plants were harvested. Cells and seedlings were cross-linked with 1% (v/v) formaldehyde for 10 min in ice and quenched by 0.125 M Gly for 5 min. The remaining steps of ChIP assays were performed as described previously with some modifications (Gendrel et al., 2005; Gao et al., 2013). In both cases, TOE1-HA was immunoprecipitated with anti-HA antibodies (Abcam). Chromatin precipitated without antibodies was used as a negative control, and the chromatin isolated before precipitation was used as an input control. Three independent biological repeats were performed. Primers used in this study are listed in Supplemental Table 3.

Seedling Growth Inhibition Assay

Arabidopsis plants were grown on 1/2 MS plates for 1 d, transferred to 1/2 MS plates containing 1 μM flg22, and then grown for another 5 d. All experiments were repeated three to four times with reproducible results.

Pathogen Assay

The pathogen assay was performed as described previously with modifications (Schreiber et al., 2008). *Pseudomonas syringae* pv *tomato* strain DC3000 was grown overnight at 28°C in King's B medium with 50 μg/mL rifampicin. Bacteria were collected, washed, and diluted to the desired density with 1/2 MS liquid medium ($OD_{600} = 5 \times 10^{-4}$). Plants were grown in 1/2 MS liquid medium for 2 d on a 12-well tissue culture plate, and then the liquid medium was replaced with the bacterial solution. Three days after inoculation, plants were ground in water, and serial dilutions were plated on King's B medium with 50 μg/mL rifamycin. The plates were incubated at 28°C for 2 d, and then bacterial colony-forming units were counted.

Replicates of Experiments and Statistical Analysis

The replicates of immunoblotting are shown in Supplemental Data Set 3. All data were analyzed using SigmaPlot 10.0 (Systat Software). The averages and SD of all results were calculated, and one-way ANOVA and Student's *t* tests were performed using GraphPad Prism 5 to generate P values. Statistically significant differences are indicated with asterisks as follows: *, $P < 0.05$; **, $P < 0.01$; and ***, $P < 0.001$. The statistical analysis of qPCR and other data is shown in Supplemental Tables 4 and 5.

ACCESSION NUMBERS

Sequence data from this article can be found in GenBank (https://www.ncbi.nlm.nih.gov/gene/) and TAIR (http://www.arabidopsis.org/) under the following accession numbers: *FLS2*, NP_199445.1, At5g46330; *TOE1*, NP_565674.1, At2g28550; *TOE2*, NP_200820, At5g60120; *MIR172B*, NR_142746, At5g04275; *AP2*, NP_195410.1, At4g36920; *PER4*, NP_172906.1, At1g14540; *CPD*, NP_196188.1, At5g05690; *BR6OX2*,

NP_566852.1, At3g30180; *EIN3*, NP_188713.1, At3g20770; *FRK1*, NP_179509.1, At2G19190; and *ARR3*, NP_176202.1, At1g59940. The RNA-seq data were deposited in the Gene Expression Omnibus database (GSE119325) at the National Center for Biotechnology Information. Mutants used in this article can be obtained from the ABRC under the following accession numbers: *toe1-2* (SALK_069677) and *toe2-1* (SALK_065370).

SUPPLEMENTAL DATA

Supplemental Figure 1. The Growth of Arabidopsis Plants during the First Week after Germination.

Supplemental Figure 2. Transcriptomic Analyses of Transcription Factor Genes Differentially Expressed during Seedling Development.

Supplemental Figure 3. Schematic Representation of the Constructs *ProFLS2*:*LUC*, *ProFLS2*:*GFP*, *TF-HA*, *ACTIN-HA*, and *ACTIN-FLAG*.

Supplemental Figure 4. Validation of the Functionality of the Protoplast Cell-Based Screening System.

Supplemental Figure 5. Screening of Transcription Factors That Can Suppress *FLS2* Promoter Activity.

Supplemental Figure 6. TOE1/2 Suppressed *FLS2* Promoter Activity.

Supplemental Figure 7. TOE1 Suppressed *EFR* Promoter Activity.

Supplemental Figure 8. TOE1 Cannot Bind to Motif 2/3 in the F-2 Fragment of the *FLS2* Promoter.

Supplemental Figure 9. EMSA Competitions with the TBS-Like Motif as a Competitor.

Supplemental Figure 10. The Growth of *Pro35S*:*FLS2-YFP-HA/fls2* Plants during the First Week after Germination.

Supplemental Figure 11. The Expression of *TOE1/2* upon PAMP Treatment at Adult Plant Stages.

Supplemental Figure 12. Analysis of *TOE1* Promoter Activity during Seedling Development.

Supplemental Figure 13. Analysis of *TOE1* Promoter Activity upon flg22 Treatment.

Supplemental Figure 14. Flg22-Induced Gene Induction in 2-d-old *miR172b* OE Plants.

Supplemental Figure 15. Level of Mature miRNA172a/b Was Increased during Seedling Development.

Supplemental Figure 16. Levels of *pre-miR172b* and Mature miR172 Were Increased upon flg22 Treatment.

Supplemental Figure 17. Analysis of *FLS2* Expression in *MIM172* Transgenic Plants.

Supplemental Figure 18. Analysis of *TOE1/2* Expression in *MIM172* Transgenic Plants.

Supplemental Figure 19. *TOE1/2* are Downregulated in *miR172b* OE Plants.

Supplemental Table 1. Primers Used for RT-qPCR.

Supplemental Table 2. Probes Used for EMSA.

Supplemental Table 3. Primers Used for ChIP-PCR.

Supplemental Table 4. ANOVA Tables.

Supplemental Table 5. Student's *t* Test Tables.

Supplemental Data Set 1. Differentially Expressed Transcription Factor Genes during Early Plant Growth as Determined by RNA-seq.

Supplemental Data Set 2. Primers Used for Construction and Genotyping.

Supplemental Data Set 3. Original Blot Images and Replicates of Immunoblotting.

ACKNOWLEDGMENTS

We thank Ping He and Libo Shan (Texas A&M University) for critical reading of the manuscript, R. Scott Poethig (University of Pennsylvania) for the *35S*::*miR172b* seeds, Xia Li (Huazhong Agricultural University) for *toe1-2* and *toe2-1* seeds, and Jiawei Wang (Chinese Academy of Sciences) and Detlef Weigel (Max Planck Institute for Developmental Biology) for *MIM172* seeds. This work was supported by the Chinese Ministry of Science and Technology (2015CB910200), the National Natural Science Foundation of China (31500990 and 31322009), and the State Key Laboratory of Plant Genomics of China.

AUTHOR CONTRIBUTIONS

D.L. conceived the project. Y.Zo., S.W., D.T., and D.L. designed research. Y.Zo., S.W., Y.Zho., J.B., G.H., X.L., and Y.Zha. performed research. Y.Zo., S.W., D.T., and D.L. analyzed data. D.L., Y.Zo., and S.W. wrote the article.

Received April 11, 2018; revised September 27, 2018; accepted October 18, 2018; published October 18, 2018.

REFERENCES

Albrecht, C., Boutrot, F., Segonzac, C., Schwessinger, B., Gimenez-Ibanez, S., Chinchilla, D., Rathjen, J.P., de Vries, S.C., and Zipfel, C. (2012). Brassinosteroids inhibit pathogen-associated molecular pattern-triggered immune signaling independent of the receptor kinase BAK1. Proc. Natl. Acad. Sci. USA **109:** 303–308.

Aukerman, M.J., and Sakai, H. (2003). Regulation of flowering time and floral organ identity by a microRNA and its APETALA2-like target genes. Plant Cell **15:** 2730–2741.

Belkhadir, Y., Jaillais, Y., Epple, P., Balsemão-Pires, E., Dangl, J.L., and Chory, J. (2012). Brassinosteroids modulate the efficiency of plant immune responses to microbe-associated molecular patterns. Proc. Natl. Acad. Sci. USA **109:** 297–302.

Boutrot, F., Segonzac, C., Chang, K.N., Qiao, H., Ecker, J.R., Zipfel, C., and Rathjen, J.P. (2010). Direct transcriptional control of the Arabidopsis immune receptor FLS2 by the ethylene-dependent transcription factors EIN3 and EIL1. Proc. Natl. Acad. Sci. USA **107:** 14502–14507.

Chen, X. (2004). A microRNA as a translational repressor of APETALA2 in Arabidopsis flower development. Science **303:** 2022–2025.

Chen, C., Ridzon, D.A., Broomer, A.J., Zhou, Z., Lee, D.H., Nguyen, J.T., Barbisin, M., Xu, N.L., Mahuvakar, V.R., Andersen, M.R., Lao, K.Q., and Livak, K.J., et al. (2005). Real-time quantification of microRNAs by stem-loop RT-PCR. Nucleic Acids Res. **33:** e179.

Chinchilla, D., Zipfel, C., Robatzek, S., Kemmerling, B., Nürnberger, T., Jones, J.D.G., Felix, G., and Boller, T. (2007). A flagellin-induced complex of the receptor FLS2 and BAK1 initiates plant defence. Nature **448:** 497–500.

Dodds, P.N., and Rathjen, J.P. (2010). Plant immunity: Towards an integrated view of plant-pathogen interactions. Nat. Rev. Genet. **11:** 539–548.

Gao, X., Chen, X., Lin, W., Chen, S., Lu, D., Niu, Y., Li, L., Cheng, C., McCormack, M., Sheen, J., Shan, L., and He, P. (2013). Bifurcation of Arabidopsis NLR immune signaling via Ca^{2+}-dependent protein kinases. PLoS Pathog. **9:** e1003127.

Gendrel, A.V., Lippman, Z., Martienssen, R., and Colot, V. (2005). Profiling histone modification patterns in plants using genomic tiling microarrays. Nat. Methods **2:** 213–218.

Gómez-Gómez, L., and Boller, T. (2000). FLS2: An LRR receptor-like kinase involved in the perception of the bacterial elicitor flagellin in Arabidopsis. Mol. Cell **5:** 1003–1011.

Halter, T., Imkampe, J., Mazzotta, S., Wierzba, M., Postel, S., Bücherl, C., Kiefer, C., Stahl, M., Chinchilla, D., Wang, X., Nürnberger, T., and Zipfel, C., et al. (2014). The leucine-rich repeat receptor kinase BIR2 is a negative regulator of BAK1 in plant immunity. Curr. Biol. **24:** 134–143.

Hann, D.R., Domínguez-Ferreras, A., Motyka, V., Dobrev, P.I., Schornack, S., Jehle, A., Felix, G., Chinchilla, D., Rathjen, J.P., and Boller, T. (2014). The Pseudomonas type III effector HopQ1 activates cytokinin signaling and interferes with plant innate immunity. New Phytol. **201:** 585–598.

Heese, A., Hann, D.R., Gimenez-Ibanez, S., Jones, A.M.E., He, K., Li, J., Schroeder, J.I., Peck, S.C., and Rathjen, J.P. (2007). The receptor-like kinase SERK3/BAK1 is a central regulator of innate immunity in plants. Proc. Natl. Acad. Sci. USA **104:** 12217–12222.

Jofuku, K.D., den Boer, B.G.W., Van Montagu, M., and Okamuro, J.K. (1994). Control of Arabidopsis flower and seed development by the homeotic gene APETALA2. Plant Cell **6:** 1211–1225.

Jones, J.D.G., and Dangl, J.L. (2006). The plant immune system. Nature **444:** 323–329.

Jung, J.H., Seo, Y.H., Seo, P.J., Reyes, J.L., Yun, J., Chua, N.H., and Park, C.M. (2007). The GIGANTEA-regulated microRNA172 mediates photoperiodic flowering independent of CONSTANS in Arabidopsis. Plant Cell **19:** 2736–2748.

Kadota, Y., Sklenar, J., Derbyshire, P., Stransfeld, L., Asai, S., Ntoukakis, V., Jones, J.D.G., Shirasu, K., Menke, F., Jones, A., and Zipfel, C. (2014). Direct regulation of the NADPH oxidase RBOHD by the PRR-associated kinase BIK1 during plant immunity. Mol. Cell **54:** 43–55.

Kardailsky, I., Shukla, V.K., Ahn, J.H., Dagenais, N., Christensen, S.K., Nguyen, J.T., Chory, J., Harrison, M.J., and Weigel, D. (1999). Activation tagging of the floral inducer FT. Science **286:** 1962–1965.

Korves, T.M., and Bergelson, J. (2003). A developmental response to pathogen infection in Arabidopsis. Plant Physiol. **133:** 339–347.

Kulcheski, F.R., Marcelino-Guimaraes, F.C., Nepomuceno, A.L., Abdelnoor, R.V., and Margis, R. (2010). The use of microRNAs as reference genes for quantitative polymerase chain reaction in soybean. Anal. Biochem. **406:** 185–192.

Li, L., Li, M., Yu, L., Zhou, Z., Liang, X., Liu, Z., Cai, G., Gao, L., Zhang, X., Wang, Y., Chen, S., and Zhou, J.M. (2014). The FLS2-associated kinase BIK1 directly phosphorylates the NADPH oxidase RbohD to control plant immunity. Cell Host Microbe **15:** 329–338.

Liang, X., Ding, P., Lian, K., Wang, J., Ma, M., Li, L., Li, L., Li, M., Zhang, X., Chen, S., Zhang, Y., and Zhou, J.M. (2016). Arabidopsis heterotrimeric G proteins regulate immunity by directly coupling to the FLS2 receptor. eLife **5:** e13568.

Lozano-Durán, R., Macho, A.P., Boutrot, F., Segonzac, C., Somssich, I.E., and Zipfel, C. (2013). The transcriptional regulator BZR1 mediates trade-off between plant innate immunity and growth. eLife **2:** e00983.

Lu, D., Wu, S., Gao, X., Zhang, Y., Shan, L., and He, P. (2010). A receptor-like cytoplasmic kinase, BIK1, associates with a flagellin receptor complex to initiate plant innate immunity. Proc. Natl. Acad. Sci. USA **107:** 496–501.

Lu, D., Lin, W., Gao, X., Wu, S., Cheng, C., Avila, J., Heese, A., Devarenne, T.P., He, P., and Shan, L. (2011). Direct ubiquitination of pattern recognition receptor FLS2 attenuates plant innate immunity. Science **332:** 1439–1442.

Lyons, R., Rusu, A., Stiller, J., Powell, J., Manners, J.M., and Kazan, K. (2015). Investigating the association between flowering time and defense in the *Arabidopsis thaliana-Fusarium oxysporum* interaction. PLoS ONE **10:** e0127699.

Malinovsky, F.G., Batoux, M., Schwessinger, B., Youn, J.H., Stransfeld, L., Win, J., Kim, S.K., and Zipfel, C. (2014). Antagonistic regulation of growth and immunity by the Arabidopsis basic helix-loop-helix transcription factor homolog of brassinosteroid enhanced expression2 interacting with increased leaf inclination1 binding bHLH1. Plant Physiol. **164:** 1443–1455.

Monaghan, J., Matschi, S., Shorinola, O., Rovenich, H., Matei, A., Segonzac, C., Malinovsky, F.G., Rathjen, J.P., MacLean, D., Romeis, T., and Zipfel, C. (2014). The calcium-dependent protein kinase CPK28 buffers plant immunity and regulates BIK1 turnover. Cell Host Microbe **16:** 605–615.

Naseem, M., Kaltdorf, M., and Dandekar, T. (2015). The nexus between growth and defence signalling: Auxin and cytokinin modulate plant immune response pathways. J. Exp. Bot. **66:** 4885–4896.

O'Malley, R.C., Huang, S.C., Song, L., Lewsey, M.G., Bartlett, A., Nery, J.R., Galli, M., Gallavotti, A., and Ecker, J.R. (2016). Cistrome and epicistrome features shape the regulatory DNA landscape. Cell **165:** 1280–1292.

Saur, I.M.L., Kadota, Y., Sklenar, J., Holton, N.J., Smakowska, E., Belkhadir, Y., Zipfel, C., and Rathjen, J.P. (2016). NbCSPR underlies age-dependent immune responses to bacterial cold shock protein in Nicotiana benthamiana. Proc. Natl. Acad. Sci. USA **113:** 3389–3394.

Schmid, M., Uhlenhaut, N.H., Godard, F., Demar, M., Bressan, R., Weigel, D., and Lohmann, J.U. (2003). Dissection of floral induction pathways using global expression analysis. Development **130:** 6001–6012.

Schreiber, K., Ckurshumova, W., Peek, J., and Desveaux, D. (2008). A high-throughput chemical screen for resistance to *Pseudomonas syringae* in Arabidopsis. Plant J. **54:** 522–531.

Schwab, R., Palatnik, J.F., Riester, M., Schommer, C., Schmid, M., and Weigel, D. (2005). Specific effects of microRNAs on the plant transcriptome. Dev. Cell **8:** 517–527.

Segonzac, C., Macho, A.P., Sanmartín, M., Ntoukakis, V., Sánchez-Serrano, J.J., and Zipfel, C. (2014). Negative control of BAK1 by protein phosphatase 2A during plant innate immunity. EMBO J. **33:** 2069–2079.

Shan, L., He, P., Li, J., Heese, A., Peck, S.C., Nürnberger, T., Martin, G.B., and Sheen, J. (2008). Bacterial effectors target the common signaling partner BAK1 to disrupt multiple MAMP receptor-signaling complexes and impede plant immunity. Cell Host Microbe **4:** 17–27.

Shi, H., Shen, Q., Qi, Y., Yan, H., Nie, H., Chen, Y., Zhao, T., Katagiri, F., and Tang, D. (2013). BR-SIGNALING KINASE1 physically associates with FLAGELLIN SENSING2 and regulates plant innate immunity in Arabidopsis. Plant Cell **25:** 1143–1157.

Stegmann, M., Monaghan, J., Smakowska-Luzan, E., Rovenich, H., Lehner, A., Holton, N., Belkhadir, Y., and Zipfel, C. (2017). The receptor kinase FER is a RALF-regulated scaffold controlling plant immune signaling. Science **355:** 287–289.

Sun, J., Xu, Y., Ye, S., Jiang, H., Chen, Q., Liu, F., Zhou, W., Chen, R., Li, X., Tietz, O., Wu, X., and Cohen, J.D., et al. (2009). Arabidopsis ASA1 is important for jasmonate-mediated regulation of auxin biosynthesis and transport during lateral root formation. Plant Cell **21:** 1495–1511.

Takeuchi, O., and Akira, S. (2010). Pattern recognition receptors and inflammation. Cell **140:** 805–820.

Tang, D., Wang, G., and Zhou, J.M. (2017). Receptor kinases in plant-pathogen interactions: More than pattern recognition. Plant Cell **29:** 618–637.

Todesco, M., Rubio-Somoza, I., Paz-Ares, J., and Weigel, D. (2010). A collection of target mimics for comprehensive analysis of microRNA function in *Arabidopsis thaliana*. PLoS Genet. **6:** e1001031.

Trapnell, C., Pachter, L., and Salzberg, S.L. (2009). TopHat: Discovering splice junctions with RNA-Seq. Bioinformatics **25:** 1105–1111.

Wang, J., Grubb, L.E., Wang, J., Liang, X., Li, L., Gao, C., Ma, M., Feng, F., Li, M., Li, L., Zhang, X., and Yu, F., et al. (2018). A regulatory module controlling homeostasis of a plant immune kinase. Mol. Cell **69:** 493–504.e6.

Wu, G., Park, M.Y., Conway, S.R., Wang, J.W., Weigel, D., and Poethig, R.S. (2009). The sequential action of miR156 and miR172 regulates developmental timing in Arabidopsis. Cell **138:** 750–759.

Xiao, Y.H., Yin, M.H., Hou, L., Luo, M., and Pei, Y. (2007). Asymmetric overlap extension PCR method bypassing intermediate purification and the amplification of wild-type template in site-directed mutagenesis. Biotechnol. Lett. **29:** 925–930.

Xing, D.H., Lai, Z.B., Zheng, Z.Y., Vinod, K.M., Fan, B.F., and Chen, Z.X. (2008). Stress- and pathogen-induced Arabidopsis WRKY48 is a transcriptional activator that represses plant basal defense. Mol. Plant **1:** 459–470.

Yoo, S.D., Cho, Y.H., and Sheen, J. (2007). Arabidopsis mesophyll protoplasts: A versatile cell system for transient gene expression analysis. Nat. Protoc. **2:** 1565–1572.

Zhai, Q., Zhang, X., Wu, F., Feng, H., Deng, L., Xu, L., Zhang, M., Wang, Q., and Li, C. (2015). Transcriptional mechanism of jasmonate receptor COI1-mediated delay of flowering time in Arabidopsis. Plant Cell **27:** 2814–2828.

Zhang, B., Wang, L., Zeng, L., Zhang, C., and Ma, H. (2015). Arabidopsis TOE proteins convey a photoperiodic signal to antagonize CONSTANS and regulate flowering time. Genes Dev. **29:** 975–987.

Zhang, J., Li, W., Xiang, T., Liu, Z., Laluk, K., Ding, X., Zou, Y., Gao, M., Zhang, X., Chen, S., Mengiste, T., and Zhang, Y., et al. (2010). Receptor-like cytoplasmic kinases integrate signaling from multiple plant immune receptors and are targeted by a *Pseudomonas syringae* effector. Cell Host Microbe **7:** 290–301.

Zhao, J., Fu, J., Li, X., Xu, C., and Wang, S. (2009). Dissection of the factors affecting development-controlled and race-specific disease resistance conferred by leucine-rich repeat receptor kinase-type R genes in rice. Theor. Appl. Genet. **119:** 231–239.

Zhong, S., Shi, H., Xue, C., Wei, N., Guo, H., and Deng, X.W. (2014). Ethylene-orchestrated circuitry coordinates a seedling's response to soil cover and etiolated growth. Proc. Natl. Acad. Sci. USA **111:** 3913–3920.

Zipfel, C., Kunze, G., Chinchilla, D., Caniard, A., Jones, J.D., Boller, T., and Felix, G. (2006). Perception of the bacterial PAMP EF-Tu by the receptor EFR restricts Agrobacterium-mediated transformation. Cell **125:** 749–760.